Self-Assembled Monolayers of Heme Derivatives on a Gold Surface

Kazutoshi Kobayashi,*,# Shin'ichiro Imabayashi,† Katsuhiko Fujita,## Kazuhide Nonaka,† Takashi Kakiuchi,†,### Hiroyuki Sasabe,#### and Wolfgang Knoll#####

Frontier Research Program, The Institute of Physical and Chemical Research (RIKEN), Hirosawa 2-1, Wako, Saitama 351-0198

†Faculty of Engineering, Yokohama National University, Tokiwadai 79-5, Hodogaya-ku, Yokohama 240-8501

(Received March 29, 2000)

Thiolated heme derivatives were synthesized and their self-assembly behaviors on gold surfaces together with that of native heme were studied. The kinetics of this adsorption and the thickness of the formed monolayer were investigated by surface plasmon resonance spectroscopy. Native heme shows a different adsorption behavior compared to that of the synthesized derivatives. Though the heme derivatives were found to form monolayers, native heme formed only irregular aggregates on gold surfaces. IR spectroscopy was used to reveal the molecular structure of the adsorbates in the vicinity of the peptide linkage in the heme molecules on the gold surfaces. UV spectroscopy was employed to determine the tilt angle of the porphyrin rings relative to the gold surface normal. Cyclic voltammograms and potential-modulated UV-vis reflectance spectra of heme derivatives were observed in order to estimate the adsorbed amount and the redox behaviors of heme derivatives on gold surfaces.

Self-assembled monolayers (SAMs) of organosulfur compounds on metal surfaces have been widely studied because of their extensive applications in molecular technologies.[1,2] Thiols and disulfides covalently adsorb onto gold surfaces through a sulfur–gold linkage, leading to the formation of highly ordered SAMs. Although the best investigated SAMs are those prepared from alkanethiolates on gold surfaces, functionalized alkanethiolate SAMs containing, e.g., ferrocenyl,[3,4] biotinyl,[5,6] 2,2′-bipyridyl,[7] and azobenzene-4,4′-diyl[8] moieties were also extensively characterized as well as ω-functionalized (e.g. –COOH, $-CONH_2$, and NH_2) SAMs for further modifications of the surfaces.[2] SAMs of the host compounds, such as cyclodextrins and calixarenes on gold surfaces, have also attracted much attention for recognition chemistry.[9—12]

Heme (iron protoporphyrin IX), which contains an iron bound to the pyrrole rings, is well known as a prosthetic group of many proteins, such as hemoglobin, myoglobin, catalase, and b-type cytochromes.[13] One important function of the heme groups is to bind oxygen using the fifth and sixth coordination positions in hemoglobin and myoglobin, in which heme is non-covalently bound to the polypeptide (apo-protein) chain through coordination bonds.

Forming SAMs of heme molecules on gold surfaces enables us not only to study the details of the reconstitution with apo-protein, but also to search for device applications, such as electrochemical bio-sensors or as modules in bio-electronics. The reconstitution reaction of heme derivatives with apo-protein on gold surfaces provides a convenient means to fabricate well-ordered protein monolayers on solid substrates, as a first step for the structural analysis of proteins and also for device applications.[14,15] One of the expected functions of a SAM of heme on a gold surface is electron transfer to the electrode via the redox-active monolayer.[4,16,17] A comparison of the redox behavior of heme in solution and on a gold surface will provide a physical basis for a better understanding of the electron-transfer reactions in molecular assemblies. Uosaki et al. reported on the construction of a very efficient electron-transfer system using a porphyrin–ferrocene–thiol system on gold.[4] Another expected function for this SAM is the electrocatalytic reduction of dioxygen as an attractive reaction for use in fuel cells,[18—20] as well as that of hydrogen peroxide.[21]

Generally, two different strategies are employed for the formation of SAMs of functional components on gold surfaces. One is a direct adsorption method of thiolated compounds, via the direct attachment of a sulfur moiety to the molecule by a synthetic procedure prior to the SAM formation step.[4] The other is covalent attachments of the func-

Present address: National Institute of Sericultural and Entomological Science, Ministry of Agriculture, Forestry, and Fisheries, Owashi 1-2, Tsukuba, Ibaraki 305-8634, Japan.
Present address: Department of Applied Science for Electronics and Materials, Graduate School of Engineering Sciences, Kyushu University, Kasuga, Fukuoka 816-8580, Japan.
Present address: Department of Energy and Hydrocarbon Chemistry, Graduate School of Engineering, Kyoto University, Kyoto 606-8501, Japan.
Present address: Department of Photonics Materials Science, Chitose Institute of Science and Technology, Bibi 758-65, Chitose, Hokkaido 066-8655, Japan.
Max-Planck-Institut für Polymerforschung, Ackermannweg 10, D-55128 Mainz, Germany

tional components onto a preformed SAM of ω-functionalized (e.g. –COOH, NH_2) alkanethiols.[21] Arifuku et al. reported that hemin immobilized on a glassy carbon electrode via an amide linkage catalyzes the electrochemical reduction of dioxygen.[20] Lötzbeyer et al. prepared hemin monolayers via an amide linkage on a modified gold surface where the cystamine was pre-covered, and reported the catalytic reduction of hydrogen peroxide.[21] In either case, they focused on the functions of hemin modified monolayers on substrates studied by electrochemical methods. The structure of that interface was still unknown. We report on the adsorption behavior and structural characterization of SAMs of thiolated heme derivatives on gold surfaces. Surface plasmon resonance spectroscopy (SPS) was utilized to estimate the optical thickness of the monolayer and to study the adsorption kinetics. Fourier-transform infrared reflection absorption spectroscopy (FTIR-RAS) and ultraviolet-visible-spectroscopy in the reflection mode (UV-vis-RAS) were utilized to estimate the structure of the adsorbed heme derivatives on gold. Cyclic voltammograms (CV) and potential-modulated UV-vis reflectance (electro-reflectance, ER) spectra of heme derivatives were observed to estimate the adsorbed amount and the redox behavior of heme derivatives on gold surfaces.

Experimental

Materials. Hemin (iron protoporphyrin IX chloride) was purchased from Funakoshi, Japan. 1-(3-Dimethylaminopropyl)-3-ethylcarbodiimide (EDC) and 4-dimethylaminopyridine (4-DMAP) were purchased from Tokyo Kasei, Japan. *N,N*-Dimethylformamide (DMF), ethanol, 2,2′-dithiobis(ethylamine) dihydrochloride (DTEA), 10,10′-dithiobis(decylamine) dihydrobromide (DTDA), chloroform, methanol, dichloromethane, sodium hydrogencarbonate, and 1 M-hydrochloric acid were purchased from Kanto Chemical, Japan (1 M = 1 mol dm^{-3}). All chemicals were used without further purification. Gold (99.999%) was purchased from Furuya Metal, Japan, and used for SPS, FT-IR, and UV-vis measurements. Gold (99.99%) was purchased from Tanaka Kikinzoku Kogyo, Japan, and used for CV and ER measurements. Mica was purchased from Nirako, Japan. Glass slides (LaSFN9 for SPS and quartz for IR and UV) were purchased from S & J Trading Inc., USA and Fujiwara, Japan, respectively.

The synthetic route of heme derivatives together with their structures is shown in Scheme 1. Native heme, thioethylated heme derivative, and thiodecylalted heme derivative are abbreviated as NH, TEH, and TDH, respectively. EDC (5.5 mmol), 4-DMAP (11 mmol), and either DTEA (5 mmol) or DTDA (5 mmol) were dissolved into DMF at R.T., and then hemin in DMF was gently added. The reaction mixture was kept at R.T. for 36 h under stirring to complete the reaction. This reaction was monitored by thin-layer chromatography (Merck), using either 8 : 2 of chloroform and methanol for TDH or 83 : 15 of chloroform and methanol for TEH as solvents, respectively. The reaction mixture was filtrated and evaporated. The residue was dissolved in dichloromethane, and then washed with 1 M-hydrochloric acid, Milli Q, and 5% sodium hydrogencarbonate. The products were purified by silica-gel (63—200 μm) chromatography (Merck), using the same solvents as in thin-layer chromatography. After purification, IR and the fast atom bombardment (FAB) mass spectra were measured to confirm the chemical structure of the heme derivatives. ν_{max} (KBr) 3295, 3085, 2922, 2850, 1644, 1547, 1460, 1438, 1377, 1337, 1306—729 cm^{-1}. *m/z* (FAB, positive mode, matrix: 3-nitrobenzyl alcohol) for TEH; Found: *m/z* 732.1. Calcd for TEH: M, 732.8. *m/z* for TDH; Found: *m/z* 957.5. Calcd for TDH: M, 957.2.

Sample Preparation. Glass slides were cleaned in 5% Extran in Milli Q water, carefully rinsed with Milli Q water, and then cleaned in ethanol. The slides were then dried in a nitrogen stream and placed in an Edwards Auto 360 evaporator. A gold film of 50 nm thickness on LaSFN9 was deposited and used for an SPS measurement. A gold film of 200 nm thickness on quartz was deposited and used for IR and UV-vis measurements. SAMs for SPS measurements were formed by applying known concentrations of the heme derivatives into an SPS flow cell equipped with gold substrates. SAMs for IR and UV-vis measurements were formed by the immersion of gold substrates in ethanol solutions of various heme derivatives for 24 h at R.T. The substrates were rinsed twice with ethanol and then dried. A gold film of several hundreds of nanometer thickness was evaporated onto freshly cleaved mica and used for CV and ER measurements.[22]

SPS Measurement. SPS measurements were carried out using a home-made experimental set-up with a Kretschmann configuration.[23—25] A He–Ne laser (λ = 632.8 nm, power 5 mW) was used as a light source. A Teflon® cell with an inlet and outlet

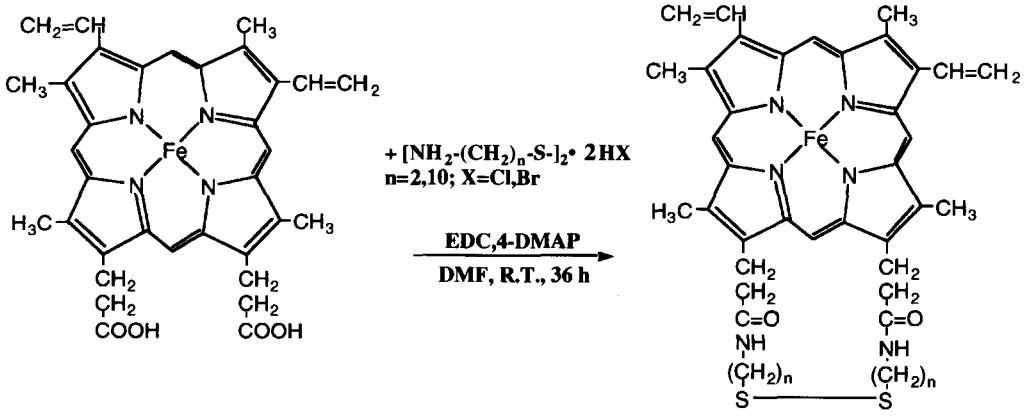

1; NH

2;n=2, TEH,
3;n=10, TDH

Scheme 1. The synthesis of heme derivatives and their structures used in this study.

ports was used for immersing the substrate to measure the kinetics on the gold surface. The reflectivity as a function of the incident angle was recorded before and after SAM formation on the substrate. These spectra were then used to determine the optical thickness of the SAMs by comparing them with a simulation based on Fresnel formulas. For a kinetic measurement, the incident angle was fixed at an angle of 0.5° smaller than the angle for the surface plasmon resonance observed as a dip in the spectra, and the reflection intensity was monitored as a function of time. We chose to evaluate our data using one refractive index (n = 1.5) for all compounds, which is often adopted for organic thin layers having no absorption bands in the considered range of wavelength.[6]

FTIR-RAS Measurement. FTIR-RAS of the SAMs were taken in the reflection mode (incident angle: 80° to the surface normal) using p-polarized light with a Mattson Infinity Series, 60AR.[26,27] The spectrometer was purged with dry nitrogen, and a liquid-nitrogen-cooled mercury–cadmium–telluride (MCT) detector was used for the reflection measurements. The spectra were recorded at 4 cm^{-1} resolution with 1024 scans. The bare gold substrate was used as a reference and cleaned just before the measurements with ethanol.

UV-vis Measurement. The absorption spectra of the heme compounds in ethanol solution were measured with an U-2000 spectrophotometer (Hitachi) using an optical cell with a 1 cm path length.

UV-vis-RAS of SAMs were taken in a reflection mode using the beam of a V-560 (JASCO) spectrophotometer at an incident angle of 45° relative to the surface normal. The optical density of the SAM was determined using a reference signal recorded with an untreated gold substrate prepared otherwise in the same way, and is denoted as $-\log(R/R_0)$, where R and R_0 are the reflectance with and without the SAM on the surface, respectively.

CV and ER Measurements. Gold substrates were immersed in ethanol containing a 50 μM solution of the different heme derivatives, taken out from the solution, rinsed with ethanol, and dried in air, successively. Though the immersion time was altered from 1 to 40 h, the peak areas and the peak potentials of the CVs for the heme derivatives depended little on the immersion time. A gold substrate onto which a SAM of a heme derivative was adsorbed was mounted in a home-made three-electrode cell using an elastic o-ring, whose diameter was 8 mm for cyclic voltammetry and 19.5 mm for ER spectroscopy. CVs and ER spectra of heme derivatives adsorbed on gold were measured in a deaerated aqueous solution of 30 mM sodium phosphate buffer, pH 7.0, at 20±3°C. The potential was referred to a Ag|AgCl| saturated KCl electrode. The instrumentation for ER measurements was described previously.[28]

Results and Discussion

The adsorption processes, the behavior of the kinetics and the final thickness of the SAMs, were followed in situ by SPS. Figure 1 shows the adsorption behaviors of NH, TEH, and TDH, respectively. The layer thickness for all samples changed quickly with a steep slope at the beginning of adsorption, showing the high affinity of heme compounds to the gold surface. The curves for TEH and TDH show then a slower process, presumably owing to the rearrangement of the adsorbed molecules on the gold surface. In order to observe only the covalently bound molecules, in situ rinsing experiments were performed. The arrows in the figure indicate the start point of the rinsing (desorption) with ethanol. However, both curves did not show any clear change in thickness. We therefore conclude that TEH and TDH are able to form well-defined monolayers on gold surfaces. On the other hand, NH exhibits quite different assembly kinetics compared to that of the heme derivatives. NH did not reach saturation in thickness, even after 24 h (data are not shown). Here, we obviously observed molecules at the surface, which are physisorbed on top of the monolayer. The film became thicker and thicker, showing NH forms aggregates. An additional adlayer of physisorbed heme molecules must be the reason for this increase in thickness. Rinsing could remove a certain amount of the physisorbed molecules.

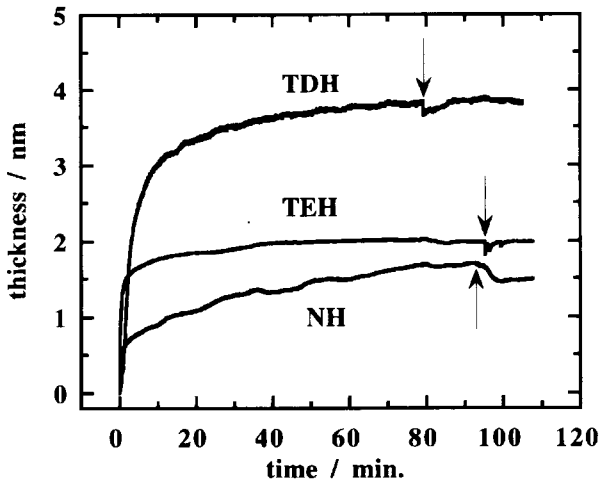

Fig. 1. In situ surface plasmon adsorption kinetics measurements for NH, TEH, and TDH. 75 μM of ethanol solution was introduced into a flow cell coupled to the surface plasmon spectrometer at 23 °C. The measured reflectivity at a constant angle of incidence was transformed into a layer thickness. Arrow shows the start of rinsing (desorption).

The influence of the initial solution concentration on the adsorption kinetics and layer thickness was measured by SPS for TDH solutions ranging from a concentration of 25 μM to 75 μM. The result is shown in Fig. 2. The adsorption profiles show that the level of adsorption increases up to a solution concentration of 50 μM, above which the initial concentration does not significantly influence the final thickness of the adsorbed heme derivatives. TEH had a similar adsorption behavior to that of TDH (data not shown). This concentration dependence on the adsorbed amount is very typical for the adsorption of thiol compounds.[29] Therefore, we used 50 μM as the initial concentration for all samples in all subsequent experiments.

Since the FT-IR measurements at grazing incidence with polarized light are sensitive to the orientation of the molecules in the SAMs, we can obtain the tilt angle of the molecules relative to the substrates.[8,26,27] Figure 3 shows the FTIR-RAS of the SAMs for TEH and TDH. Two characteristic bands of amide I (1650 cm^{-1}) and amide II (1540 cm^{-1}) were observed in this region, although these peaks were observed at 1644 and 1547 cm^{-1} in the transmission spectra taken in KBr pellets (see the Experimental section). The peak of amide I has its origin in the CO stretching mode

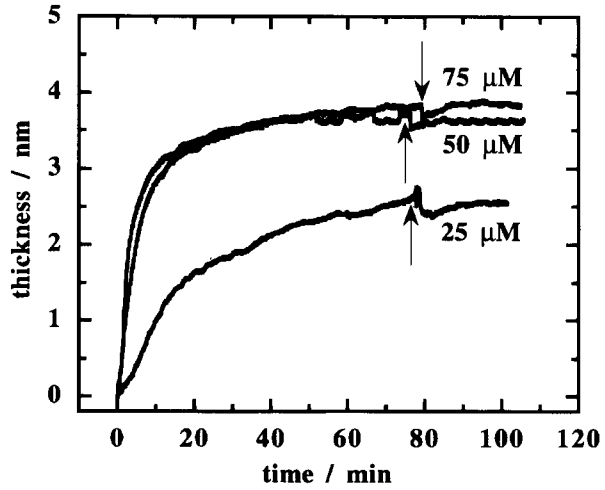

Fig. 2. In situ surface plasmon adsorption kinetics measurements for TDH. 75 μM, 50 μM, and 25 μM of ethanol solution were introduced into the flow cell of the surface plasmon spectrometer at 23 °C. Reflectivity at a constant angle of incidence was transformed into a layer thickness. Arrow shows the start of rinsing (desorption).

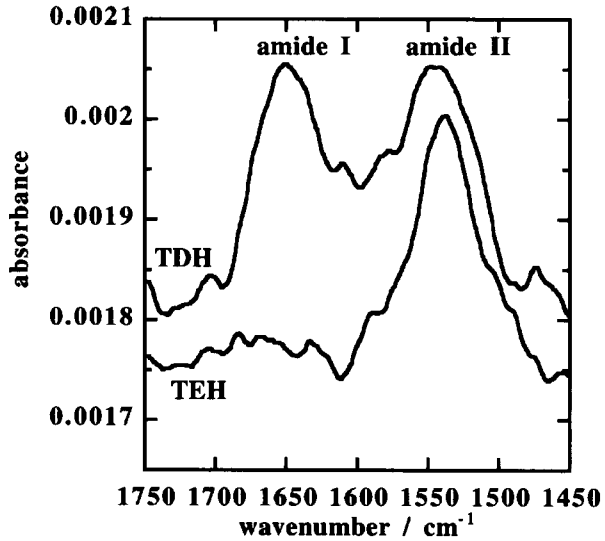

Fig. 3. IR-RAS scans (1450—1750 cm^{-1}) of monolayers of TEH and TDH on gold substrates. A bare gold substrate served as a reference. The heme derivatives (50 μM in ethanol) were adsorbed for 24 h at 23 °C.

and that of amide II in the CN stretching and NH bending. The difference in the intensity ratio of these two peaks can be explained in terms of the orientation of the peptide linkage in the heme derivatives on the gold substrate. In an FTIR-RAS experiment, the absorption bands ascribed to a transition moment perpendicular to the surface become intensive. On the other hand, a transition moment of the amide I band in heme derivatives is directed perpendicular to the molecular axis of the molecules. Compared to that, the transition moment of the amide II band in heme derivatives is directed parallel to the molecular axis of the molecules. Therefore, heme derivatives should be oriented with a smaller angle away from the surface normal when the intensity ratio of amide I to amide II is smaller. Since the spectrum of the SAM of TEH did not show any clear absorption of amide I compared to that of amide II, TEH molecules are found to be adsorbed normal to the surface with a very small tilt angle. On the other hand, the spectrum of the SAM of TDH clearly showed the absorption of both amide I and amide II, showing that TDH molecules adsorb on the gold surface with a certain tilt angle to it. We did not attempt a quantitative analysis of these IR data to determine the average tilt angles of heme derivatives in the SAMs on the gold surfaces, because it is unreasonable to assume that the amide planes of the derivatives are parallel to their molecular axes and are freely rotating.

Since the absorptions of amide I and amide II originated in the peptide linkage, we probably could deduce the adsorbed structure in the vicinity of the peptide linkage in the heme molecules by FTIR-RAS measurements. Therefore, we utilized UV-vis-RAS to clarify the adsorbed structure of heme derivatives in the vicinity of the porphyrin rings. The dotted curves in Fig. 4 show the UV-vis spectra for NH, TEH, and TDH, respectively, in ethanol solution. These spectra have absorption bands at around 400 nm due to the Soret band in the oxidized state. Figure 4 displays the UV-vis-RAS of SAMs for NH, TEH, and TDH adsorbed on gold substrates, measured in air at an incident angle of 45°. It seems that there exist two bands: one at 420 nm and the other at 520 nm. However, detailed examinations by Tsuboi et al.[30] and Fujita et al.[31] revealed that the peaks at around 520 nm do not originate from the absorption of thiolated compounds adsorbed on the gold surface, but from the characteristics of the refractive index of gold in the examined wavelength region. The anomaly of the refractive index of gold at around 520 nm produces a ghost peak. Actually, Tsuboi et al. could show a similar absorption even in an alkanethiol SAM that possesses no absorption in the corresponding region.[30] The peak at around 520 nm is inevitable in studies of thiolated compounds on gold surfaces by reflection spectroscopy. Therefore, the peak at around 520 nm in Fig. 4 was neglected in our analysis. UV-vis-RAS using polarized light was used to determine the tilt angles of the porphyrin rings of heme derivatives in SAMs on gold surfaces. Yoneyama et al. first introduced this method to examine the orientation of phthalocyanine molecules in Langmuir–Blodgett films.[32] Luk et al.,[33] Azumi et al.,[34] and Aramata et al.,[35] employed this method to clarify the molecular ordering of porphyrins, and succeeded in determining the tilt angles of the molecules in the films. The peak positions of the Soret band in the SAMs compared to those in solution were red-shifted. This suggests that the electronic interaction among heme molecules was stronger in the SAMs than in solution.[35–37] The orientation of heme molecules in the SAMs (tilt angle, ϕ, between the transition moment of the molecules and the surface normal) was calculated according to the literature using the following equation[32–35]

$$A_s/A_p = \sin^2\phi/(\cos^2\beta\sin^2\phi + 2\sin^2\beta\cos^2\phi), \quad (1)$$

where A_s is the absorption intensity measured using *s*-polar-

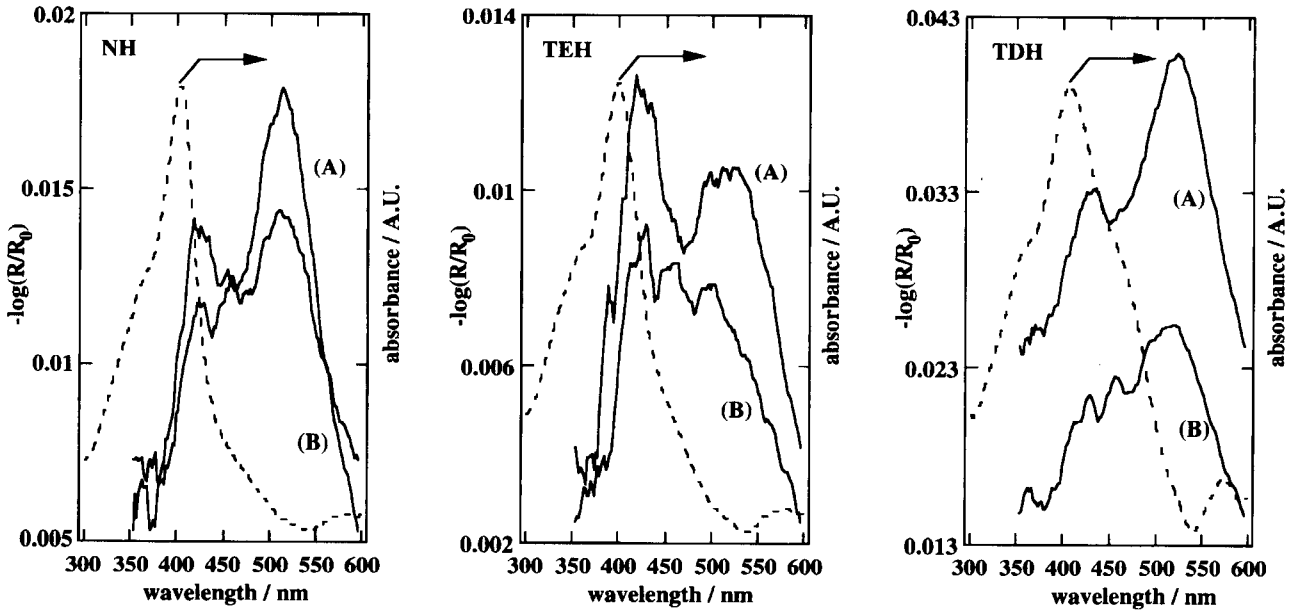

Fig. 4. UV-vis-RAS scans for heme derivatives. The reflection spectra were collected using *p*- (A) and *s*- (B) polarized light incident at 45° with respect to the surface normal. A bare gold substrate served as a reference. The heme derivatives (50 μM in ethanol) were adsorbed on the gold substrates for 24 h at 23 °C. The dotted curves represent the UV-vis spectra of NH, TEH, and TDH in ethanol solution.

ized light, A_p the absorption intensity measured using *p*-polarized light, and β the refraction angle inside the monolayer for 45° incidence. The value, $\beta = 28.1°$, was calculated, assuming a refractive index of $n = 1.5$ for all compounds. Therefore, the angle ϕ can be calculated from the experimental values of A_s and A_p. For NH, the value ϕ was calculated to be 46°, which is probably the average angle, because the NH forms aggregates, and this aggregation should occur without a certain direction against the substrates. The calculated values of ϕ for TEH and TDH were 41° and 37°, respectively. Putting the obtained results by IR and UV spectroscopy together gives us the schematic illustration shown in Fig. 5. Although the layer thickness expected from the tilt angles and the molecular lengths are larger than those estimated by SPS (Fig. 1), this could result from an overestimation of the refraction index and the electron density for the SAM layers due to the structural disorder or orientational anisotropy.

We now turn to the electrochemical characterization of the SAMs. Figure 6 shows CVs for NH, TEH, and TDH adsorbed on gold/mica electrodes. Only one peak appeared around −0.35 V for the heme derivatives, whereas two peaks were observed at −0.05 and −0.35 V for NH. The peak potential, $E_p = -0.35$ V, coincides with the reported values for the E_ps of hemin covalently bound to the amine terminal groups of thiols modified on a gold electrode[21,38] and hemin adsorbed on a pyrolytic graphite electrode.[39] The origin of the peak at −0.05 V for NH is not well understood, although the ER data represent that this peak arises from heme groups adsorbed on gold (data not shown). For all CVs, the cathodic peak current was proportional to the sweep rate, revealing that the redox response arises from the surface-confined species. The area of the cathodic peak tends to be larger than that of the anodic peak for all CVs, and this reflects the contribution of the catalytic reduction current of dioxygen, which remained in the buffer solution even after deaeration. With repeated potential sweeps between +0.3 and −0.6 V for TEH, the cathodic peak gradually decreased and the area of both the cathodic and anodic peaks became almost equal, as shown in Fig. 7. The initial reduction peak was restored within 15 min between CV measurements, indicating that the reduction in the cathodic peak mentioned above, indeed, resulted from a depletion of dioxygen in the vicinity of the electrode surface, due to the repetitive reduction of dioxygen.

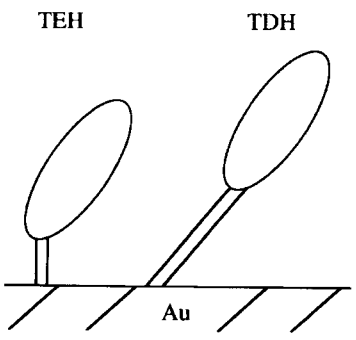

Fig. 5. Models for the structures of the heme derivatives on the gold surfaces.

The amount of redox-active heme groups on gold estimated from the cathodic peak area after repeated potential sweeps was 4.4×10^{-11} mol cm^{-2} for TEH, and 2.7×10^{-11} mol cm^{-2} for TDH. The theoretical monolayer coverage for heme was derived to be 7.0×10^{-11} mol cm^{-2}, assuming an area of 2.38 nm^2 for one heme.[40] In the case of a close-packed monolayer of perpendicularly orientated heme to the electrode surface, an order of magnitude greater than that for a

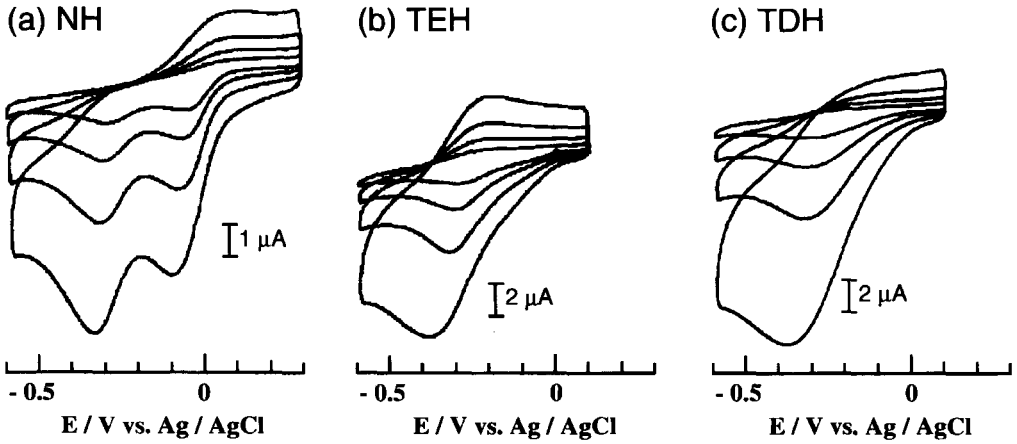

Fig. 6. Cyclic voltammograms of (a) NH, (b) TEH, and (c) TDH adsorbed on Au(111) in 30 mM sodium phosphate: scan rate, 20, 50, 100, 200 mV s^{-1}; initial potential, +0.1 V for TEH and TDH, +0.3 V for NH.

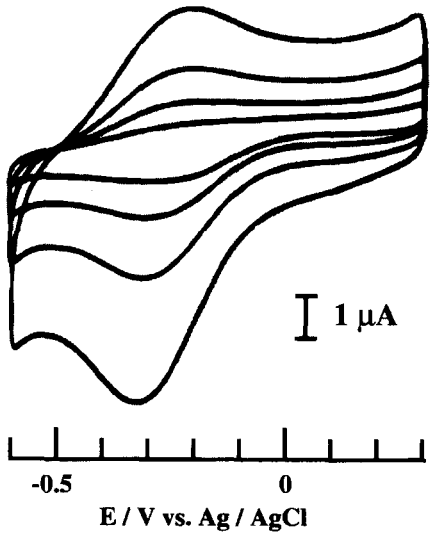

Fig. 7. Cyclic voltammograms of TEH adsorbed on Au(111) in 30 mM sodium phosphate measured after the repetitive potential sweeps: scan rate, 20, 50, 100, 200 mV s^{-1}; initial potential, +0.3 V.

flat orientation is expected. The values obtained for the heme derivatives were significantly smaller than those values, indicating the formation of less closely packed monolayers of the heme derivatives or the presence of electro-inactive heme groups. No significant change in the peak potential and the amount of redox-active heme groups was observed by increasing the adsorption time of the heme derivatives beyond 1 h. This shows that the adsorption of the heme derivatives was almost finished within 1 h, which is consistent with the adsorption behavior obtained from the SPS measurements. The smaller CV response for TDH suggests that the heme derivative with longer side chains is difficult to form a dense single-component monolayer.

While the CV peak area remained constant after the heme derivative-coated gold electrode was left in the buffer solution for 20 h, the peak area for NH decreased to 1/10 of the initial value after the CV experiments (2 h). This is consistent with the fact derived from the SPS measurements that NH is physisorbed on gold, and that the heme derivatives are covalently immobilized on gold surfaces through gold-sulfur anchoring.

Figure 8 represents the real and imaginary parts of the ER signal for TEH adsorbed on gold electrodes measured at the peak potential of the corresponding CV. TDH did not exhibit any ER response. Although the reason for no ER response for TDH is not totally clear, one possible explanation is slow electron-transfer (ET) rate for TDH in which the heme groups are on average far apart from the electrode surface compared with that of TEH.[28] The similarity of the ER spectra of TEH to a difference absorption spectrum between the reduced and oxidized forms of NH in solution supports the interpretation that the redox response originates from the adsorbed heme moieties on gold. However, both the positive and negative peaks in the ER spectra, which originate from the reduced and oxidized states of the heme, respectively,

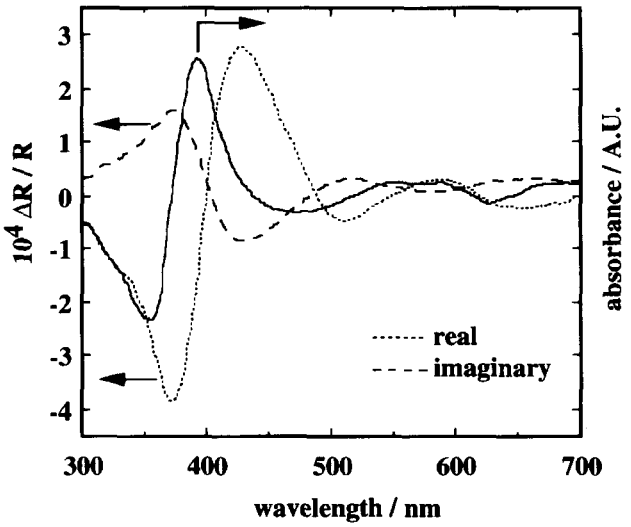

Fig. 8. ER spectra of TEH adsorbed on Au(111) in 30 mM sodium phosphate: $E_{dc} = -0.30$ V, freguency = 8 Hz, modulation amplitude = 50 mV. The solid line shows a difference absorption spectrum between the reduced and the oxidized forms of NH in the bulk solution.

shifted by about 10—20 nm toward a longer wavelength than the corresponding peaks of the difference absorption spectrum, revealing the presence of electronic interactions among the heme groups in the SAM.

The ratio of the magnitude of real and imaginary components, which is a measure of the magnitude of the electron transfer rate constant, k_{ET},[28] reveals that the k_{ET} for TEH is higher than that for NH. This suggests that the thiolate side chains allow the immobilization of heme groups in an orientation appropriate for ET to the gold electrode. From the frequency dependence of the ER response,[41] $k_{ET} = 600\ s^{-1}$ was estimated for TEH adsorbed on gold. The k_{ET} values for heme and heme-containing substances adsorbed on electrode surfaces alter over a wide range, depending on the immobilization manner. Lötzbeyer et al. obtained $k_{ET} > 30\ s^{-1}$ for the hemin bound to the amine groups of 2-aminoethanethiol modified on gold electrode from CV measurements.[21] The order of $10^3\ s^{-1}$ was estimated for the k_{ET} of cytochrome *c* immobilized on COOH-terminated thiolate SAMs in which the number of methylene units is lower than 8.[42] Ruzgas et al. determined that the k_{ET} of microperoxidase-11, which consists of a polypeptide of 11 amino residues attached covalently to the heme, immobilized on gold in a monolayer state is more than $1000\ s^{-1}$.[43] Compared with these reported values, the k_{ET} value obtained in this work is reasonable, and it is concluded that the heme groups in TEH are suitable for rapid heterogeneous ET.

In summary, we have demonstrated and quantified the adsorption behavior of native heme and its thiolated derivatives on gold surfaces using SPS, IR, and UV spectroscopies, and have also characterized their redox behavior using CV and ER methods. The results given in this study will be particularly useful for device applications.[4,16—21] In order to fabricate well-ordered protein monolayers on gold surfaces by the reconstitution of the heme derivatives with apo-protein, which is one of the goals of our research, an appropriate distance is needed between each heme group in order to accommodate the larger size of the peptide chains compared with the heme derivatives. By dilution of the heme derivatives with thiol compounds, it should be possible to form an appropriate monolayer of heme derivatives optimized for the reconstitution reaction. The formation of SAMs from reconstituted heme proteins will be published elsewhere.

We would like to thank Drs. Masahiko Hara and Takashi Isoshima (The Institute of Physical and Chemical Research, RIKEN) and Dr. Kotaro Kajikawa (Tokyo Institute of Technology) for helpful discussion and UV-vis measurement.

References

1 A. Ulman, "An Introduction to Ultrathin Organic Films:From Langmuir–Blodgett to Self-Assembly," Academic Press, Boston (1991).

2 A. Ulman, *Chem. Rev.*, **96**, 1533 (1996).

3 M. Yanagida, T. Kanai, X. -Q. Zhang, T. Kondo, and K. Uosaki, *Bull. Chem. Soc. Jpn.*, **71**, 2555 (1998).

4 K. Uosaki, T. Kondo, X. -Q. Zhang, and M. Yanagida, *J. Am. Chem. Soc.*, **119**, 8367 (1997).

5 J. Spinke, M. Liley, F. -J. Schmitt, H. -J. Guder, L. Angermaier, and W. Knoll, *J. Chem. Phys.*, **99**, 7012 (1993).

6 J. Spinke, M. Liley, H. -J. Guder, L. Angermaier, and W. Knoll, *Langmuir*, **9**, 1821 (1993).

7 Y. S. Obeng and A. J. Bard, *Langmuir*, **7**,195 (1991).

8 K. Tamada, J. Nagasawa, F. Nakanishi, K. Abe, M. Hara, W. Knoll, T. Ishida, H. Fukushima, S. Miyashita, T. Usui, T. Koini, and T. R. Lee, *Thin Solid Films*, **150-155**, 327 (1998).

9 M. Weisser, G. Nelles, P. Wohlfart, G. Wenz, and S. Mittler-Neher, *J. Phys. Chem.*, **100**, 17893 (1996).

10 Y. Maeda and H. Kitano, *J. Phys. Chem.*, **99**, 487 (1995).

11 F. Davis, A. J. Lucke, K. A. Smith, and C. J. M. Stirling, *Langmuir*, **14**, 4180 (1998).

12 A. Friggeri, F. C. J. M. van Veggel, and D. N. Reinhoudt, *Langmuir*, **14**, 5457 (1998).

13 L. Stryer, "Biochemistry," 3rd ed, W. H. Freeman and Company, New York (1988).

14 K. Kobayashi, T. Nagamune, T. Furuno, and H. Sasabe, *Bull. Chem. Soc. Jpn.*, **72**, 691 (1999).

15 L. -H. Guo, G. McLendon, H. Razafitrimo, and Y. Gao, *J. Mater. Chem.*, **6**, 369 (1996).

16 C. E. D. Chidsey, *Science*, **251**, 919 (1991).

17 L. Jiang, A. Glidle, C. J. McNeil, and J. M. Cooper, *Biosens. Bioelectron.*, **12**, 1143 (1997).

18 P. A. Forshey and T. Kuwana, *Inorg. Chem.*, **22**, 699 (1983).

19 J. Zak, H. Yuan, M. Ho, L. K. Woo, and M. D. Porter, *Langmuir*, **9**, 2772 (1993).

20 F. Arifuku, T. Saeki, and H. Kurihara, *Fukuoka Univ. Sci. Rep.*, **23**, 63 (1993).

21 T. Lötzbeyer, W. Schuhmann, and H. -L. Schmidt, *J. Electroanal. Chem.*, **395**, 341 (1995).

22 S. Imabayashi, M. Iida, D. Hobara, Z. Q. Feng, K. Niki, and T. Kakiuchi, *J. Electroanal. Chem.*, **428**, 33 (1997).

23 W. Knoll, *MRS Bull.*, **7**, 29 (1991).

24 J. M. Phelpes and D. M. Taylor, *J. Phys. D: Appl. Phys.*, **1996**, 1080.

25 E. Kretschmann, *Z. Phys.*, **241**, 313 (1971).

26 K. Tamada, J. Nagasawa, F. Nakanishi, K. Abe, T. Ishida, M. Hara, and W. Knoll, *Langmuir*, **14**, 3264 (1998).

27 K. Fujita, N. Bunjes, K. Nakajima, M. Hara, H. Sasabe, and W. Knoll, *Langmuir*, **14**, 6167 (1998).

28 T. Sagara, S. Igarashi, H. Sato, and K. Niki, *Langmuir*, **7**, 1005 (1991).

29 C. D. Bain, E. B. Troughton, Y. -T. Tao, J. Evall, G. M. Whitesides, and R. G. Nuzzo, *J. Am. Chem. Soc.*, **111**, 321 (1989).

30 K. Tsuboi, K. Kajikawa, N. Hamada, K. Fujita, M. Hara, H. Sasabe, W. Knoll, K. Seki, and Y. Ouchi, *Mol. Cryst. Liq. Cryst.*, **322**, 191 (1998).

31 K. Fujita, M. Hara, H. Sasabe, W. Knoll, K. Tsuboi, K. Kajikawa, K. Seki, and Y. Ouchi, *Langmuir*, **14**, 7456 (1998).

32 M. Yoneyama, M. Sugi, M. Saito, K. Ikegami, S. Kuroda, and S. Iizima, *Jpn. J. Appl. Phys.*, **25**, 961 (1986).

33 S. Y. Luk, F. R. Mayers, and J. O. Williams, *Thin Solid Films*, **157**, 69 (1988).

34 R. Azumi, M. Matsumoto, Y. Kawabata, S. Kuroda, M. Sugi, L. G. King, and M. J. Crossley, *J. Phys. Chem.*, **97**, 12862 (1993).

35 K. Aramata, M. Kamachi, M. Takahashi, and A. Yamagishi, *Langmuir*, **13**, 5161 (1997).

36 J. A. Bergeron, G. L. Gaines, and W. D. Bellamy, *J. Colloid Interface Sci.*, **25**, 97 (1967).

37 R. B. Beswick and C. W. Pitt, *Chem. Phys. Lett.*, **143**, 589 (1988).

38 H. Zimmermann, A. Lindgern, W. Schuhmann, and L. Gorton, *Chem. Eur. J.*, **6**, 592 (2000).

39 T. Sagara, S. Takagi, and K. Niki, *J. Electroanal. Chem.*, **349**, 159 (1993).

40 C. F. Kolpin and H. S. Swofford, Jr., *Anal. Chem.*, **50**, 916 (1978).

41 Z. Q. Feng, T. Sagara, and K. Niki, *Anal. Chem.*, **67**, 3564 (1995).

42 Z. Q. Feng, S. Imabayashi, T. Kakiuchi, and K. Niki, *J. Chem. Soc., Faraday Trans.*, **93**, 1367 (1997).

43 T. Ruzgas, A. Gaigalas, and L. Gorton, *J. Electroanal. Chem.*, **469**, 123 (1999).